Impact behaviour of 3-layered metal-polymer-metal sandwich panels

Chiara Colombo [a,*], Adele Carradó [b], Heinz Palkowski [c], Laura Vergani [a]

[a] Politecnico di Milano, Department of Mechanical Engineering, Via La Masa 1, 20156 Milano, Italy
[b] Université de Strasbourg, Institut de Physique et Chimie des Matériaux de Strasbourg, CNRS UMR 7504, 23 rue du Loess, 67000 Strasbourg, France
[c] Clausthal University of Technology (TUC), IMET Institute of Metallurgy, Robert-Koch-Strasse 42, 38678 Clausthal-Zellerfeld, Germany

1. Introduction

Sandwich composites are a particular class of composite materials combining two or more mono-material layers with different physical and mechanical properties. They generally present outer stiffer skins made of steel or aluminium alloys sheets with an inner core of a homogeneous or structured polymer layer, or fibre reinforced plastics. Sandwich composites have recently found wide applications in many industrial fields such as the automotive one but also in aviation and marine areas, aiming to manufacture lightweight but stiff and performing structures [1,2].

These composites have, in fact, many interesting features. First of all, they can be easily manufactured and they are characterised by a high specific strength, a good sound-deadening and damping, as well as impact resistance and good formability. Besides, their characteristics can be improved and tailored to the specific needs, by varying combination and thickness of layers.

* Corresponding author.
E-mail addresses: chiara.colombo@polimi.it (C. Colombo), adele.carrado@ipcms.unistra.fr (A. Carradó), heinz.palkowski@tu-clausthal.de (H. Palkowski), laura.vergani@polimi.it (L. Vergani).

An example of application of such sandwich panels is the automotive hood consisting of two aluminium or steel skins combined with a polypropylene (PP) core (Hylite®) or two steel layers with a polyamide (PA) core [2–5]. Focusing on steel metal sheets as reinforcement layers, some studies were proposed on panels made of high-grade austenitic stainless steel (316L) cover sheets and a core of a polyolefin (PP/PE), which is a polypropylene (PP) and polyethylene (PE) blend [6–8], or even with titanium cover sheets for biomedical or aviation applications [9]. A number of combinations in thickness and steel material were investigated to understand the influence of these material and geometrical changes on the forming limits of these hybrids compared to the metallic mono-materials [9].

It is important to know the mechanical properties of these sandwich composites for their final application. For instance, formability is one of the main information required when designing the shape of automotive components [10], but it is also a property affecting their behaviour when subjected to impacts [11].

Focusing on the application of sandwich panels in the automotive field, important issues are low velocity impacts of small objects, i.e. stones. This kind of event is, in fact, very frequent and it is important to evaluate its effect on the residual mechanical behaviour of the damaged panel and on the integrity and reliability of the structure where it is placed.

Nomenclature

E	elastic modulus
PE	polyethylene
PP	polypropylene
PU	polyurea
SDD	specific damage deflection, normalised with respect to impact energy
SDE	specific damage extension, normalised with respect to impact energy
YS	yielding stress
UTS	ultimate tensile strength
ε_f	elongation to failure
σ_D	damage stress identified by thermography

Scientific literature presents studies on the effect of impacts not only on metal sheets, but also on combining different coupled layers. For instance, metal sheets can be combined with fibre-reinforced layers (*i.e.* fibre-metal laminates [12–14], or with plastic layers to improve impact behaviour. Focusing on these sandwich panels, recent studies showed that polymers can increase the overall impact resistance of steel, when the polymer layer is applied on the opposite side to the impact and providing that sufficient adhesion is offered between the layers [15–17]. These studies considered experimental impact tests and numerical simulations on panels made of two layers, steel and polyurea (PU). It is stated the importance of the 1 mm thick PU layer that captures and dissipates part of the shock. In addition, if the plate does not fail during the initial shock loading, PU can increase the effective shear modulus of the bilayer plate and thus delay the onset of the necking instability. Because of these considerations, polymeric coatings of metal sheets retard the occurrence of fracture.

This behaviour is evidenced also increasing the thickness of the polymeric layer up to 12 mm, both with high [18] and low-velocity impacts [19]. In the second case, PU coated aluminium plates show a considerable reduction in out-of-plane deformation when compared to the uncoated plates, thus suggesting the possibility of using such a covering layer as an efficient energy absorbing and damping material against low velocity impact damage.

The study by [20] performed numerical analyses to check also the influence of impact on multi-layered steel plates (metal-polyurea-metal sheet). They highlighted that the cohesive strength plays an important role during impact for energy dissipa-tion, especially during the final stage of panel perforation and petalling fracture.

In the present work, attention is focused on a three-layered symmetrical metal-polymer-metal sandwich panel shown in Fig. 1. With the aim of understanding the mechanical response of this material after low-velocity impacts, experimental impact tests are carried out varying the thickness of both metal and PP/PE layers. The attention is then focused on the post-impact residual strength of the damaged panels experimentally determined by applying tensile unidirectional load.

To get more information on the behaviour of the impacted panels, the infrared thermography is applied to monitor variations in surface temperature of the specimens. Infrared thermography is a non-contact and non-destructive experimental technique, based on the concept of surface temperature scanning during the application of a mechanical or thermal load to a structural component. In the literature different methods have been developed by means of thermography, initially applied to homogeneous materials [21], and recently applied also to composite structures [22,23]. The attention is focused on the correlation between the thermal response of the material under mechanical loads, either static or dynamic, and the detection of the damage initiation. In particular, this technique can detect the damage initiation at very early stage, in correspondence of the stress at the end of thermoelastic trend, during tensile test. This stress is called damage initiation stress, σ_D [22].

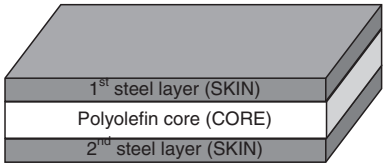

Fig. 1. Scheme of the sandwich panels.

2. Material and experimental setup

This paragraph describes materials and methods used for the experimental tests.

2.1. Sandwich panels

The sandwich panels were produced in a two-stage roll bonding process. In the first stage, after a pre-treatment of the surfaces of the metal sheets of deep drawing qualities and of the PP/PE foils, an epoxy resin (Köratec 201) with a thickness of approximately 10 μm was applied on the metal surface and cured at around 260 °C. Then, the polyolefin foil was pre-heated up to 120 °C and roll bonded to the metal cover sheet. In the second step, this "half sandwich" was roll bonded to the final sandwich panel with the pre-treated second cover sheet under appropriate conditions. More information about the pre-treatment conditions and the pro-cess is in [6].

Four types of sandwich panel with different layer thicknesses were produced as listed in Table 1. Also, two deep drawing steel grades TS245 and TH620 (EN 10027-1 standard) were used for manufacturing the panels. They both were produced by rolling, the TH620 was kept in the work hardened version and the TS245 finally recrystallization annealed. TS245 is used for panels A, C, D with higher thicknesses; TH620 is used for panel B having the thin-nest metal sheet. The mechanical properties of these steels, yield strength YS, ultimate strength UTS, elongation to rupture ε_f and Young's modulus E, are given in Table 2.

The bonding behaviour of the sandwich panels was investigated in the past by T-peel test; inner defects could be analysed by Lock-in thermography as introduced in [24].

Table 1
Sandwich panels identification.

Panel #	Steel grade	Skin thickness [mm]	Core thickness [mm]	Total thickness [mm]
A	TS245	0.49	0.6	1.58
B	TH620	0.135	0.6	0.87
C	TS245	0.24	0.6	1.08
D	TS245	0.24	0.3	0.78

Table 2
Mechanical properties from tensile test on the mono-metal sheets.

Steel grade	Thickness [mm]	YS [MPa]	UTS [MPa]	ε_f [%]	E [GPa]
TS245	0.49	215 ± 5	321 ± 9	29.8 ± 0.6	184 ± 13
TS245	0.24	193 ± 5	281 ± 20	35.4 ± 2.9	149 ± 8
TH620	0.135	498 ± 24	500 ± 25	1.5 ± 0.3	183 ± 8

2.2. Equipment for impact tests

For impact tests, plates of size 200 × 300 mm^2 with different thickness ratios and materials were used following Table 1. Fig. 2 shows the device used to perform the impact tests on the plates. It consists of a drop weight tower centred on a frame in which every panel is placed and fixed. Panels are clamped at the corners by cross-placing four bar. The dimension of the impacted square region to impact is 60 × 60 mm^2. All screws of the external frame were symmetrically fixed to avoid any disturbances during the impact. Fig. 2 also shows the mass (0.6 Kg) used for impacts. It is composed of a central steel body with a 48 mm diameter, and a spherical tip with a diameter of 25.4 mm (1 inch). This tip was hardened by quenching to avoid its damage during the test, and thus to localise all the damage on the sandwich panel. The mass is held at the initial height (1540 mm) into the pipe by a magnet, and then released and dropped by gravity.

The impact deflection of the sandwich panels depends on the thickness of the cover sheet and on its strength as well as the ratios in thickness of the layers. For this reason, the impacts are performed using the same energy for all the tests, thus the same height for the dropping mass, delivering a potential energy E_p equal to 9.06 J.

The energy value is selected since it is:

- Sufficiently high, in order to obtain a visible damage with plastic residual deformation in all the sandwich panels, in particular the one with the highest thickness (Panel A).
- As small as possible, in order to avoid perforation of the dropping mass into the panel with the lowest thickness (Panel B). The attention of the present work is indeed focussed on impact damage, but avoiding perforation.

Due to the friction between pipe wall and mass, each impact was performed with its characteristic value of kinetic energy. In order to calculate the mass speed at the impact, a laser was placed in the last part of the pipe, provided with a slit on one side (Fig. 2). The laser was connected to an acquisition system (CompactDAQ by National Instruments), sampling the displacement signals at 1 kHz. These data were transferred to a laptop by data-logging software (LabVIEW Signal Express by National Instruments), used also to analyse and plot the signal as a function of time. Knowing mass length and time, it is possible to define the mass speed and to estimate the kinetic energy E_k of each impact. The average value of E_k is (6.39 ± 1.01) J. This means that around 30% of the potential energy is lost into the impacting system due to friction (E_k/E_p = 70%).

2.3. Measurements of the residual deformation

After the impacts, depth of the induced damage is analysed by means of a contact profilometre (Zeiss Prismo 5 VAST MPS HTG CMM). The head of the profilometre consists of a sphere with 1 mm diameter (accuracy: 3 μm), which is in contact with the panel. Since all the impacts are nearly symmetrical, profile measurements of residual deformation (vertical depth) are performed only along one direction, centred in the impact region. All measures were performed on the impact side. Indeed, by a visual inspection, profile trend on the rear part (opposite to the impact) was very similar to the front one. Results of these measurements were vectors of the in-line and the out-of-plane coordinates. This last coordinate was identified as the damage depth.

From profile measures, two parameters are identified (Fig. 3): Z_{max} maximum vertical residual deflection, and $L_{80\%}$ which is the measure of the width of the impression, along the in-plane direction, corresponding to $Z_{80\%}$, that is 80% of Z_{max}. This measure seemed well fitting with the diameter of a circle including the impact region.

Table 3 shows these parameters, evaluated for each type of sandwich panel. Specific quantities are also evaluated, on the basis of the kinetic impact energy as in Eq. (1):

$$\begin{aligned} \text{Specific Damage Deflection, SDD} &= \frac{Z_{max}}{E_k} \\ \text{Specific Damage Extension, SDE} &= \frac{L_{80\%}}{E_k} \end{aligned} \quad (1)$$

Comparing these results, some initial considerations can be drawn. Considering the first three sandwich panels, which have the same core thickness, the decrease in the metal thickness induces an increase in SDD. In terms of SDE, it seems that the pan-els B have a wider deformed region, which also depends on the dif-ferent steel grade.

On the contrary, considering the last two types of sandwich panels, which have the same thickness of metal layer, the decrease in core thickness also induces significant increase in the specific damage parameters (+80% in SDD and +60% in SDE, Table 3).

These quantities, and especially SDD, can be very useful to compare the different damage induced in the sandwich panels. Indeed, there is a mutual influence of thickness of the panel, ratio of the components and steel grade which seems to play an important role on residual deflection of the sandwich panels. In order to separate these factors, two normalised plots of SDD are given in Fig. 4. Fig. 4a shows SDD normalised with respect to the material strength. On the other hand, Fig. 4b plots the parameter SDD nor-malised with respect to the cover thickness. From these two plots, it is evident that sandwich panels A, C and D show a progressive increase of the deflection, with the decrease of metal thickness. Moreover, the plots evidence the performing behaviour of panel B, made of a different steel grade, when normalised with respect to strength (Fig. 4a), but not in terms of thickness (Fig. 4b).

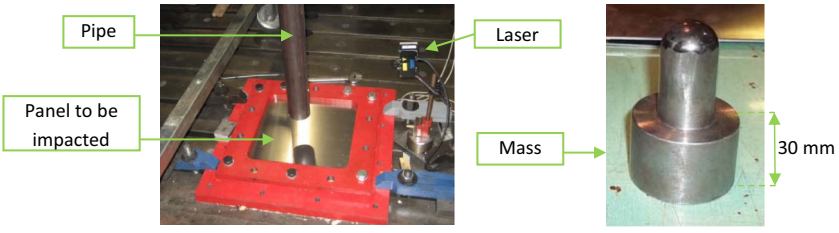

Fig. 2. Experimental device and setup for impact tests.

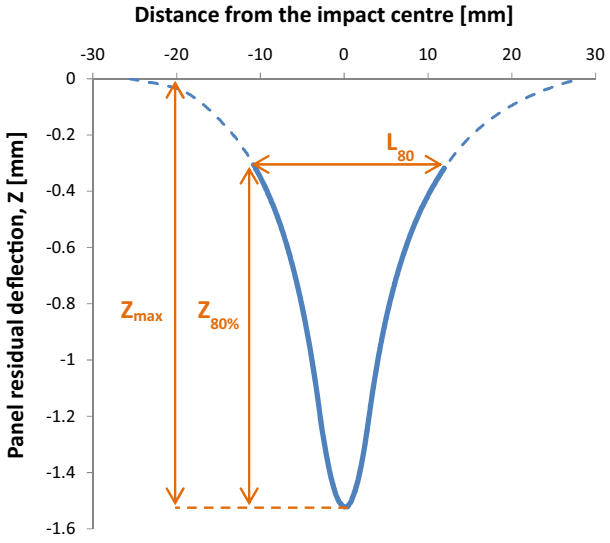

Fig. 3. Trend of the residual deflection in one of the A panels. Identification of parameters Z_{max} and $L_{80\%}$.

Table 3
Average values of the main parameters measured on each type of sandwich panel.

Panel	E_k, kinetic energy at the impact [J]	Z_{max} [mm]	$L_{80\%}$ [mm]	Specific Damage Deflection, SDD [mm/J]	Specific Damage Extension, SDE [mm/J]
A	6.62	−1.704	25.05	0.259 ± 0.014	3.822 ± 0.362
B	6.90	−1.034	31.23	0.419 ± 0.022	4.547 ± 0.532
C	5.85	−1.959	20.25	0.327 ± 0.065	3.430 ± 0.274
D	6.91	−4.020	37.83	0.582 ± 0.017	5.472 ± 0.285

3. Post-impact tensile tests

Rectangular specimens were cut from undamaged and impacted plates. Dimensions of these specimens are: 45x200 mm^2; the impact region was centred in the specimen along the in-plane directions. Six tensile tests were performed from each impacted panel.

Tensile post-impact tests were carried out by an electromechanical universal testing machine MTS Alliance RT/150 equipped with a 100 KN load cell. All tests were performed at room temperature, under standard humidity condition and with a crosshead displacement rate of 5 mm/min. All tested specimens failed in correspondence of the central region. Moreover, the failure of all the impacted specimens occurred at the damaged region.

These post-impact static tensile tests were performed not only with the aim of analysing the variation in the mechanical response of the damaged material with respect to the one in undamaged conditions, but also to relate it to the thermal response.

Indeed, any time a variation of stress that occurs in an object as a consequence of load application, a small variation of the temperature also occurs, associated with the elastic deformations. This is the so-called thermoelastic phenomenon [25]. These variations in temperature are typically very small, and only recent advances in thermal equipment and photon detectors allowed to measure them efficiently and reliably. During static tensile tests, the tem-perature trend evidences three stages: an initial temperature increase, a plateau region and then a final further increase in tem-perature [21]. Analysing this trend, a stress corresponding to the end of the thermoelastic stage, σ_D (end of the linear decreasing stage of the temperature) can be detected. According to some recent studies on composite fibre reinforced materials, it is related to the beginning of damage into the material and it is called dam-age initiation stress [22,23,26,27]. As far as the authors know, no works are present in the literature dealing with the application of this experimental technique to sandwich panels.

The apparatus for thermal analysis consists of infrared thermographic camera, type FLIR Titanium SC7000. During tensile tests, the thermal camera was placed at a distance of around 30 cm from the specimen surface. Fig. 5 shows the experimental setup during tensile tests. Thermal sensitivity of the camera is up to 20 mK. Spatial resolution of the thermal camera is 320 × 256 pixels. The acquisition frequency used for the tests was set to 20 Hz. Before testing, specimens were sprayed with a black mat lacquer to avoid problems due to different emission factors.

Fig. 6 shows area identification on specimens' surfaces for thermal data post-processing. This area selection was the same for all the tested and analysed specimens. For undamaged specimens, the whole specimen surface was selected (Area 0). From the dam-aged specimens, two circular areas with the same dimension (diameter = 12 pixels, corresponding to 7.5 mm) are selected:

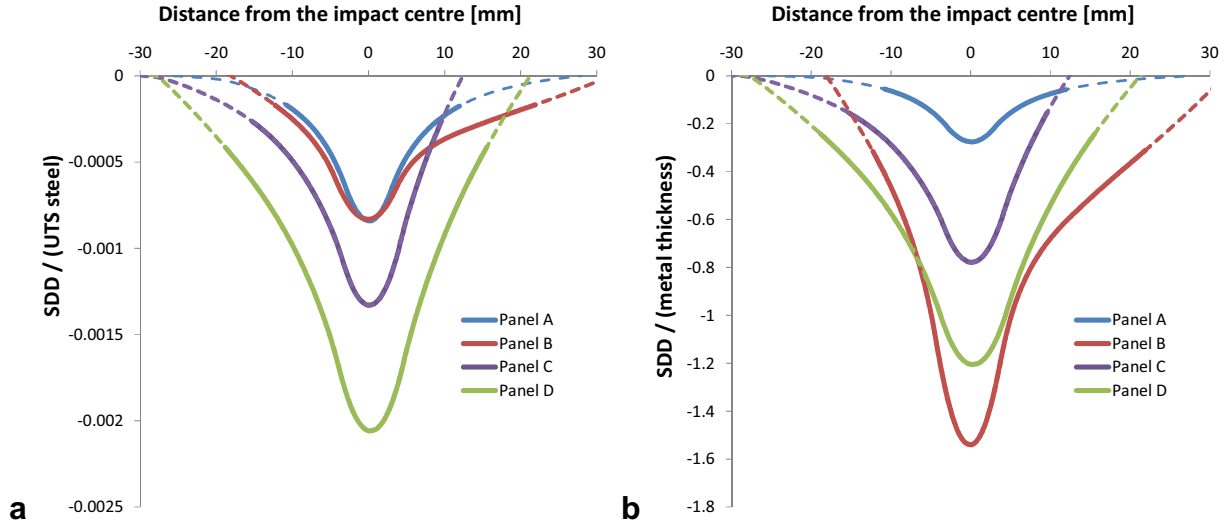

Fig. 4. Normalization of Specific Damage deflection (SDD) parameter with respect to UST of each steel cover (a) and cover metal thickness (b).

Fig. 5. Experimental setup during static tests: positioning of the thermal camera.

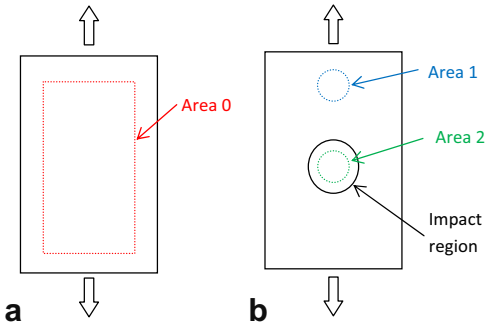

Fig. 6. Area identification for thermographic analysis in undamaged (a) and impacted specimens (b).

- Area 1, far from the damaged region, corresponding to undamaged material.
- Area 2, centred into the impact region, corresponding to damaged material.

A part of the specimens was thermally monitored from the impact side and part from the rear. Anyway, no net difference in terms of thermographic results was recorded.

3.1. Mechanical results

Fig. 7a shows the curves of the simple steel plates and Fig. 7b shows stress versus strain curves of the mechanical tests on sandwich panels, in undamaged and impacted conditions. For these last tests, no extensometer was used, due to the extended impact region and to the performed thermal measures, which will be discussed in the following paragraph. Comparing these two figures, the steel plates always experience higher values of stress but lower strain, when compared to the sandwich panels. This indicates a higher property of sandwich panels to deform under loads, compared to the single metal sheet.

These plots are very repeatable. As it can be expected, stress-strain curves coming from the same type of panel are very

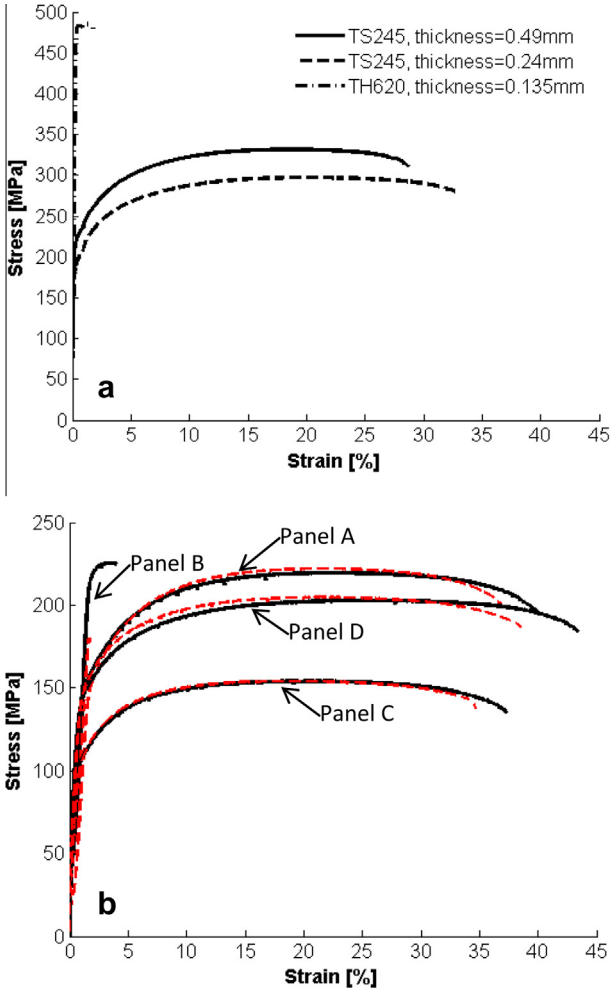

Fig. 7. Results of experimental tensile tests: stress-strain curves. (a) metal sheets;(b) undamaged (solid black line) and impacted (dashed red line) specimens for each tested panel type. (For interpretation of the references to colour in this figure legend, the reader is referred to the web version of this article.)

similar. Table 4 summarizes results from these curves in terms of yielding stress, ultimate tensile strength and elongation to rupture. In this table, very small deviation values are listed for all these mechanical quantities. However, some considerations can be drawn.

Panels B, the thinnest ones, showed in the undamaged configuration a very limited flat trend after the initial linear elastic stage as the steel sheets were not annealed after rolling. On the other hand, the impacted specimens experienced a sudden failure right at the end of the linear stage, showing a more brittle behaviour. Thus, YS coincides with UTS. This can evidence a high level of damage induced into the specimens, as a consequence of impact.

Analysing the average values of UTS and YS, Table 4 shows similar values for panels A in the damaged and undamaged configuration, having the thickest metal layers. For these sandwiches, it seems that the residual mechanical static properties are not modified by the induced damage, when compared to the undamaged configuration.

On the contrary, for panels C having lower metal thickness with respect to the previous ones, when comparing undamaged and damaged tests, values of yielding stress decreases, while UTS remains constant. For the thinnest plate, panel B, also UTS is modified by the presence of impact. These considerations are exposed in Fig. 8 for panels having the same core thickness (A, B, C). This

Table 4
Mechanical properties from tensile tests on sandwich panels.

Panel	YS [MPa]	UTS [MPa]	ε_f [%]
A, Undamaged	154	220	41.0
A, Impacted	152 ± 4	221 ± 1	39.1 ± 1.6
B, Undamaged	215	226	4.2
B, Impacted	192 ± 11	192 ± 11	1.9 ± 0.1
C, Undamaged	126	154	37.5
C, Impacted	113 ± 3	154 ± 1	35.5 ± 1.2
D, Undamaged	148.2	203	44.0
D, Impacted	151 ± 2	203 ± 2	37.8 ± 2.2

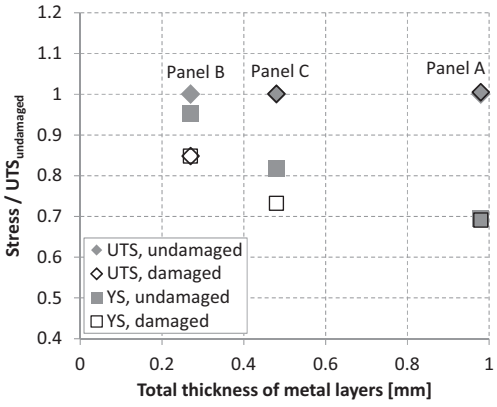

Fig. 8. Trends of YS and UTS, normalised by the corresponding UTS of the undamaged material and plotted as a function of metal layer thickness (for panels A, B, C having the same core).

figure plots stress values, normalised with respect to UTS of the undamaged specimens.

Separate consideration can be drawn for panels D, with intermediate metal thickness, and reduced core (0.3 mm instead of 0.6 mm, as all the other panels). For these specimens, it seems that neither UTS nor YS are modified by the damage presence (Table 4).

For all the stress-strain curves in Fig. 7b, comparing undamaged with damaged specimens made from sandwich panels, it results a decrease in maximum strain. In fact, local plasticity due to the impact induces the panels to have a less ductile behaviour. Moreover, it should be noted that all undamaged specimens failed at the central region, far from the grips; damaged specimens failed at the impacted region.

Fig. 9 shows a comparison in terms of the strains at failure, normalised with respect to the undamaged specimens ($\varepsilon_{f,\text{undamaged}}$). In terms of strains, sandwich panels with higher metal thicknesses illustrate a quite similar behaviour ($\varepsilon_{f,\text{damaged}}$ = 85–95% $\varepsilon_{f,\text{undamaged}}$ for panels A, C, D), while panel B with the lowest metal thickness definitely experiences a different mechanical behaviour ($\varepsilon_{f,\text{damaged}}$ = 45% $\varepsilon_{f,\text{undamaged}}$). This behaviour of panel B can be due not only to the small thickness, but also to the combined effect of the different steel grade used for the cover. From this consider-ation, also strain at failure can be identified as a parameter able to define the level of induced damage.

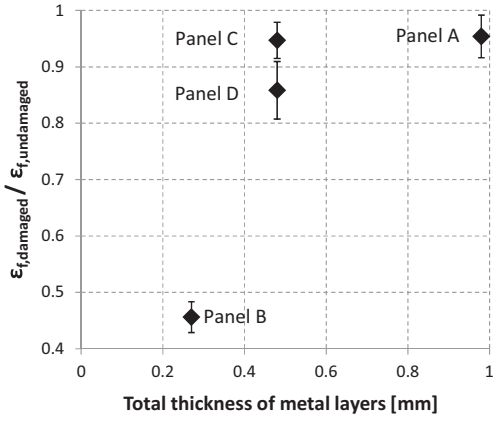

Fig. 9. Plot of normalised strains at failure as a function of total thickness of the metal layer.

3.2. Thermographic results

Before presenting the thermographic results, an example of data analysis is described for undamaged and damaged specimens of panel A.

Fig. 10 shows the plots of thermo-mechanical data from area A0 of an undamaged specimen, and from areas A1 and A2 of an impacted specimen (see Fig. 6). The stress σ versus time t trend and the corresponding temperature variation ΔT in function of time t for the whole test is given. Surface temperature variation was identified for each selected area; for instance, for area A1 it was identified as ΔT (A1).

These curves are highly reproducible and very similar for all the analysed specimens. Clearly, temperature increases during the tests in a very similar way for all specimens. Temperature increases up to 10 K, although in the area of damage and finally at failure this rate is even higher. The global heating of the speci-men is meaningful of the progressive damage created during testing.

Fig. 11 shows a magnification of the same plot presented in Fig. 10 for the initial testing time. A decreasing temperature trend at the beginning of the test is characteristic of the thermoelastic effect. After this stage, a minimum is reached, followed by an increase for the rest of the test.

Comparing undamaged and impacted specimens, a different trend is clearly visible not only from the purely mechanical quantity (σ), but also from the thermal measurement (ΔT). According to the literature, initial thermal data can be interpolated by a linear regression describing the thermoelastic effect (thermoelastic law) as in Eq. (2):

$$\Delta T = -K \cdot T_0 \cdot \Delta(\sigma_1 - \sigma_2) \tag{2}$$

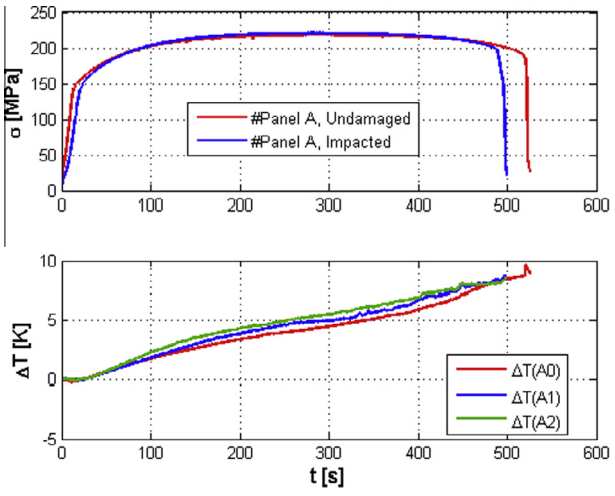

Fig. 10. (a) Stress vs time and (b) temperature variation ΔT vs time plots, for the three considered areas (0: undamaged specimen; 1: damaged specimen, undamaged region; 2: damaged specimen, impacted region).

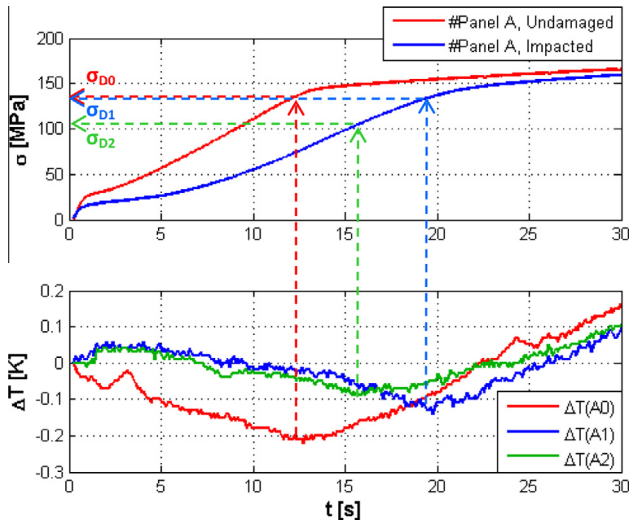

Fig. 11. Magnification of Fig. 10 at the initial testing time. Example of identification of the three σ_D.

where ΔT is the temperature variation, K is the thermoelastic constant, T_0 is the room temperature in absolute value and $\Delta(\sigma_1-\sigma_2)$ is the variation in principal surface stresses.

At the end of the thermoelastic linear stage, the damage stress σ_D [22,23,26,27] can be identified, as in Fig. 11. This stress corre-sponds to the beginning of a local damage, which is likely to occur before global yielding. In order to obtain σ_D, a linear regression interpolates initial data from ΔT–σ plot. To process data by an automatised procedure with Matlab® scripts, the proposed crite-rion for data selection is to add data to the linear regression model until the coefficient of determination R^2 increases (maximisation procedure). This coefficient is an indication of the linearity of data and should be as near to one as possible. For all the analysed set of experimental data, this value was greater than 0.9.

Fig. 12 shows a comparison between the three interpolations in a ΔT–σ plot. Slopes of these straight lines are very similar for all tested panels and there is no evident difference between undamaged and damaged panels. Slopes, indeed, are given by the product $(-K \cdot T_0)$ from Eq. (2) which is the same both for undamaged and impacted specimens. Moreover, intercepts of these straight lines (Fig. 12) are generally slightly positive for damaged specimens and around or below zero for the undamaged material.

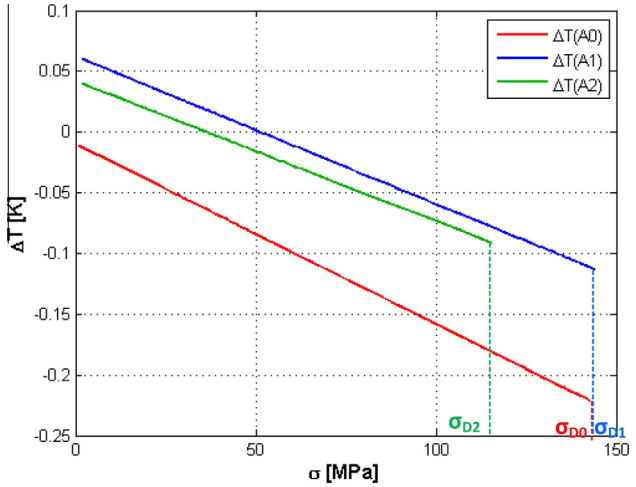

Fig. 12. Linear regressions from experimental ΔT vs stress data: comparison among A0, A1, A2.

The highest scatter for these thermal data is detected for panels D, which seem to be the most damaged.

Moreover, from Fig. 12, interpolations with linear curves in the ΔT–σ plane show different intercepts with the vertical axis. Undamaged specimen experiences an intercept almost zero, so it starts immediately cooling when the load is applied. On the contrary, the damaged specimen experiences a very small temperature increase, around 0.05 K, within 5s. This initial inversion in temperature trend seems typical of most of the damaged specimens, since impact zone influences the trends not only in the damaged A1, but also in A2 far from it. Indeed, the impacted specimens are subjected to axial and bending stresses due to the deformation of the panels. This loading condition influences the stress and temperature fields mainly at the beginning of the test, when data are also very scattered.

Finally, further considerations can be drawn in terms of the obtained damage stresses. As shown in Fig. 11 and Fig. 12, the undamaged specimen (subscript 0, red line) and undamaged area from impacted specimen (subscript 1, blue line) present curves which end up approximately in correspondence of the same stress. This signifies that damage stress σ_D and global thermo-mechanical behaviour of the sandwich panel is very similar for all the undamaged areas ($\sigma_{D0} \approx \sigma_{D1}$). On the contrary, considering damaged area from impacted specimen (subscript 2, green line), the trend shown in Fig. 12 ends at a lower σ_{D2} value. This behaviour was detected also for specimens of the other tested sandwich panels. Table 5 summarizes these mechanical and thermoelastic quantities, obtained from experimental static tensile tests. Stresses are normalised with respect to UTS.

It results that the σ_D values are always lower than the yielding stress (UTS > YS > σ_D). Hence, the damage stress value σ_D can be used to identify the presence of a local damage before yielding occurs. This consideration is valid for undamaged and damaged specimens.

Finally, comparing σ_D from the three analysed areas, there is not a unique trend among σ_{D0}, σ_{D1} and σ_{D2}. Generally we can assume that σ_{D2} is the smallest, except from the one calculated for panels D, which appeared the most scattered and damaged. For panels A, having thicker metal thickness, the difference between YS and damage stress is wider. On the contrary, decreasing metal or core thickness, this difference is reduced, and it is more difficult to detect through thermography the localised presence of damage before mechanical yielding and failure occur. This phenomenon is really evident in panel B, where the thermographic technique can detect damage only at 90% UTS. This means a more sudden fail-ure and a more brittle behaviour, since damage is already cumu-lated into the specimen.

The information of the stress σ_D, corresponding to the damage initiation and coming from thermographic analyses, is not really meaningful from the standpoint of the residual strength of impacted sandwich panels, since UTS is not modified by the impacts. However, the damage stress σ_D can be useful in the case of fatigue loads. The presence of damaged regions could be considered as a stress intensification, which localises the beginning of the

Table 5
Results of mechanical and thermographic measurements, performed during tensile static tests.

Panel	YS/UTS	σ_{D0}/UTS (undamaged specimen)	σ_{D1}/UTS (impacted specimen)	σ_{D2}/UTS (impacted specimen)
A	0.695	0.585	0.583	0.518
B	0.952	0.907	0.932	0.906
C	0.818	0.695	0.623	0.614
D	0.729	0.690	0.641	0.649

damage in the panel. This behaviour cannot be identified by classical static tests, hence the importance of thermography and its application for design and damage monitoring.

Given these considerations, thermographic technique seems to be very useful to identify damage initiation before yielding occurs in sandwich specimens, both in undamaged and impacted conditions. Indeed, the damage stresses σ_D could be a useful design parameter, able to identify the presence of a damaged region in the panel before the yielding stress occurs and to perform a non-destructive assessment of the damage progression in this type of sandwich materials.

4. Conclusions

In this work, an experimental study on post-impact behaviour of sandwich panels was presented. Different thicknesses of metal sheets and polyolefin core were considered to check their influence on the material damage and its progression during post-impact tensile tests. Thermography was used during testing to monitor the thermal response of the specimens.

From the presented results the following conclusions can be drawn. First, some parameters to identify the impact damage are:

- The specific deflection caused by the damage (SDD) and the related damaged area (SDE), which are deeply influenced by the decrease in both metal and polyolefin thickness. Indeed, a mutual influence of panel thickness, steel grade and ratio of the components induces different behaviours of sandwich panels, caused by the same impact energy.
- The strain to failure, ε_f. During the post-impact tensile tests, impacted specimens always experienced a lower ε_f, in the range 45–95% ε_f of undamaged conditions.
- The damage stress σ_D evaluated through thermographic monitoring of the specimen surface. This stress value was higher for undamaged specimens than for impacted ones. Moreover, for all the tested panels, the lowest σ_D is measured in correspondence of the impacted region.

Finally, this paper showed that the thermographic technique could be a useful and valid tool to monitor the behaviour of impacted sandwich specimens during the tensile tests. Indeed, thermal measurements allow the definition of a damage stress σ_D lower than the yielding stress. σ_D can be a useful design parameter to evaluate the damage of the impacted panels.

References

[1] Palkowski H, Sokolova OA, Carradò A. Sandwich materials. In: Crolla D, Foster DE, Kobayashi T, Vaughan N, editors. Encyclopedia of automotive engineering. John Wiley & Sons Ltd; 2013. p. 1–17.

[2] Engel B, Buhl J. Metal forming of vibration damping composite sheets. Steel Res Int 2011;82:626–31.

[3] Burchitz I, Boesenkool R, van der Zwaag S, Tassoul M. Highlights of designing with Hylite – a new material concept. Mater Des 2005;26:271–9.

[4] Kim KJ, Rhee MH, Choi BI, Kim CW, Sung CW, Han CP, et al. Development of application technique of aluminum sandwich sheets for automotive hood. Int J Precis Eng Manuf 2009;10:71–5.

[5] ThyssenKrupp Steel. Bondal® Körperschalldämpfender Verbundwerkstoff. [Online]; 2009. Available from: <www.thyssenkrupp-steel.com>.

[6] Sokolova O, Carradò A, Palkowski H. Production of customized high-strength hybrid structures. Adv Mater Res 2010;137:81–128.

[7] Sokolova OA, Carradò A, Heinz Palkowski H. Metal–polymer–metal sandwiches with local metal reinforcements: a study on formability by deep drawing and bending. Compos Struct 2011;94:1–7.

[8] Carradò A, Faerber J, Niemeyer S, Ziegmann G, Palkowski H. Metal/polymer/metal hybrid systems: towards potential formability applications. Compos Struct 2011;93:715–21.

[9] Harhash M, Carradò A, Palkowski H. Lightweight titanium/polymer/titanium sandwich sheet for technical and biomedical application. Materialwissenschaft und Werkstofftechnik 2014;45:1084–91.

[10] Kim KJ, Kim D, Choi SH, Chung K, Shin KS, Barlat F, et al. Formability of AA5182/polypropylene/AA5182 sandwich sheets. J Mater Process Technol 2003;139:1–7.

[11] Seth M, Vohnout VJ, Daehn GS. Formability of steel sheet in high velocity impact. J Mater Process Technol 2005;168:390–400.

[12] Chai GB, Manikandan P. Low velocity impact response of fibre-metal laminates – A review. Compos Struct 2014;107:363–81.

[13] Fan J, Guan ZW, Cantwell WJ. Numerical modelling of perforation failure in fibre metal laminates subjected to low velocity impact loading. Compos Struct 2011;93:2430–6.

[14] Manikandan P, Chai GB. A layer-wise behavioral study of metal based interply hybrid composites under low velocity impact load. Compos Struct 2014;117:17–31.

[15] Amini MR, Nemat-Nasser S. Micromechanisms of ductile fracturing of DH-36 steel plates under impulsive loads and influence of polyurea reinforcing. Int J Fract 2010;162:205–17.

[16] Amini MR, Isaacs JB, Nemat-Nasser S. Experimental investigation of response of monolithic and bilayer plates to impulsive loads. Int J Impact Eng 2010;37:82–9.

[17] Amini MR, Amirkhizi AV, Nemat-Nasser S. Numerical modeling of response of monolithic and bilayer plates to impulsive loads. Int J Impact Eng 2010;37:90–102.

[18] Roland CM, Fragiadakis D, Gamache RM, Casalini R. Factors influencing the ballistic impact resistance of elastomer-coated metal substrates. Philos Mag 2013;93:468–77.

[19] Mohotti D, Ngo T, Raman SN, Ali M, Mendis P. Plastic deformation of polyurea coated composite aluminium plates subjected to low velocity impact. Mater Des 2014;56:696–713.

[20] Xue L, Mock WJ, Belytschko T. Penetration of DH-36 steel plates with and without polyurea coating. Mech Mater 2010;42:981–1003.

[21] Clienti C, Fargione G, La Rosa G, Risitano A, Risitano G. A first approach to the analysis of fatigue parameters by thermal variations in static tests on plastics. Eng Fract Mech 2010;77:2158–67.

[22] Colombo C, Libonati F, Vergani L. Fatigue damage in GFRP. Int J Struct Integrity 2012;4:424–40.

[23] Colombo C, Vergani L, Burman M. Static and fatigue characterisation of new basalt fibre reinforced composites. Compos Struct 2012;94:1165–74.

[24] Palkowski H, Sokolova O, Carradó A. Reinforced metal/polymer/metal sandwich composites with improved properties. the minerals, metals & materials society. Supplemental proceedings: materials fabrication, properties, characterization, and modeling, vol. 2. Hoboken, NJ, USA: John Wiley & Sons, Inc.; 2011.

[25] Thomson W. On the thermoelastic, thermomagnetic, and pyroelectric properties of matter. Philos Mag Series 1878;5:4–27.

[26] Colombo C, Vergani L. Influence of delamination on fatigue properties of a fibreglass composite. Compos Struct 2014;107:325–33.

[27] Montesano J, Fawaz Z, Bougherara H. Non-destructive assessment of the fatigue strength and damage progression of satin woven fiber reinforced polymer matrix composites. Compos Part B: Eng 2015;71(71):122–30.